Development 112, 397-406 (1991)
Printed in Great Britain © The Company of Biologists Limited 1991



# Expression of the fibroblast growth factor-5 gene in the mouse embryo

OLIVIA HAUB and MITCHELL GOLDFARB*

*Columbia University College of Physicians and Surgeons, Department of Biochemistry and Molecular Biophysics, 630 West 168th Street, New York, NY 10032*

*To whom reprint requests should be addressed

## Summary

**Fibroblast growth factors (FGFs) are structurally related mitogens that can regulate the differentiation of a wide variety of cells. As a step towards elucidating the developmental roles played by one of these factors, we have used *in situ* hybridization methods to examine expression of the murine *Fgf-5* gene during embryogenesis. *Fgf-5* RNA was detected at seven distinct sites in the developing mouse embryo: (1) postimplantation epiblast (embryonic day 5½–7½), (2) lateral splanchnic mesoderm (E9½–10½), (3) lateral somatic mesoderm (E10½–12½), (4) myotomes (E10½–12½), (5) mastication muscle (E11½–14½), (6) limb mesenchyme (E12½–14½), and (7) acoustic ganglion (E12½–14½). At several of these sites, expression is spatially restricted within the tissues. We offer several hypotheses regarding the roles of FGF-5 in murine development.**

Key words: mouse embryo, FGF-5, fibroblast growth factor-5, RNA, *in situ* hybridization.

## Introduction

Fibroblast growth factors (FGFs) are structurally related mitogenic proteins encoded by at least seven distinct genes in mammals (Goldfarb, 1990). In addition to their growth-promoting activities towards a broad spectrum of cell types, FGFs are suspected of playing various roles in the control of cellular differentiation (reviewed in (Burgess and Maciag, 1989)). *In vitro*, the prototypic FGFs (acidic and basic FGF) can promote neuronal survival and neurite outgrowth (Hatten *et al.* 1988; Lipton *et al.* 1988; Morrison *et al.* 1986; Unsicker *et al.* 1987; Walicke *et al.* 1986; Walicke and Baird, 1988), commit sympathoadrenal progenitor cells to the sympathetic neural lineage (Birren and Anderson, 1990), regulate the development of skeletal muscle precursor cells (Lathrop *et al.* 1985; Seed and Hauschka, 1988), and induce mesodermal differentiation in amphibian blastula ectoderm (Kimelman and Kirschner, 1987; Slack *et al.* 1987). FGF *in vivo* implants can promote angiogensis (Folkman and Klagsbrun, 1987), promote the formation of new nerve fiber tracts (Thompson *et al.* 1989) and prevent retrograde degeneration of neurons in the central nervous system (Anderson *et al.* 1988). Consistent with their potential roles in development, several FGF genes are expressed at various stages of embryogenesis (reviewed in (Goldfarb, 1990)).

FGF-5 was first identified as the product of a human proto-oncogene detected by DNA transfection assays (Zhan *et al.* 1988). The growth factor is a secreted glycoprotein (Bates *et al.* 1991) that is mitogenic towards fibroblasts *in vitro* (Zhan *et al.* 1988). As a step towards understanding the native functions of this growth factor *in vivo*, we have studied the profile of mouse *Fgf-5* gene expression in adult tissues and during embryogenesis. We have previously reported the presence of *Fgf-5* RNA at low levels in the adult central nervous system and its localization within certain neurons (Haub *et al.* 1990). In this paper, we present an analysis of *Fgf-5* gene expression in the mouse embryo, as detected by *in situ* hybridization.

## Materials and methods

### *Enzymes and radionucleotides*

Enzymes for nucleic acid biochemistry were purchased from New England Biolabs, Boehringer Mannheim and Stratagene. Radiolabelled nucleotides were purchase from DuPont/New England Nuclear.

### *cDNA isolation and RNA filter blot hybridization*

A 2.2 kbp cDNA clone was isolated by screening a E11½ mouse embryonic cDNA library (Clonetech) with a murine *Fgf-5* third exon fragment (Haub *et al.* 1990). The cDNA clone extends from approximately the 50th codon in the *Fgf-5* open reading frame to near the 3′ end of the message. RNA was isolated from cells following guanidine isothiocyanate extraction (Chirgwin *et al.* 1979). CCE embryonic stem (ES) cells were provided by Dr E. Robertson and were maintained in the undifferentiated state by passage on STO fibroblast feeder layers, or were used to make embryoid bodies by

standard procedure (Martin and Evans, 1975). E6¾–E7 egg cylinders were dissected from their decidua and teased free of ectoplacental cone, which is reddish in appearance. *E. coli* RNA was added as carrier during egg cylinder RNA purification. To quantitate egg cylinder RNA, one tenth of recovered material was analyzed by RNA 'northern' filter blotting (Thomas, 1980) in comparison to a 10–1000 nanagram range of ES RNA, using rat glyceraldehyde phosphate dehydrogenase (GAPDH) cDNA (Fort *et al.* 1985) as hybridization probe. DNA probes were $^{32}$P-radiolabelled by random hexamer-primed DNA synthesis (Feinberg and Vogelstein, 1983).

### In situ *hybridization*

Radiolabelled RNA riboprobes were synthesized in standard reactions (Melton *et al.* 1984) using SP6, T3, or T7 RNA polymerase, depending upon vector DNA template. Uridine($\alpha^{35}$S-thio)triphosphate and uridine[$\alpha^{32}$P]triphosphate were incorporated to specific activities of $7\times10^8$ and $2\times10^9$ cts min$^{-1}$ $\mu$g$^{-1}$, respectively. The *Pst*I–*Sac*I fragment of *Fgf-5* DNA (Haub *et al.* 1990) (see Fig. 1) was used as template for antisense- and sense-strand riboprobes (antiPS and sensePS), and the *Pst*I–*Pst*I cDNA fragment was used to make antisense probe (antiPP) to corroborate hybridization data. A plasmid containing 120 base pairs of non-coding first exon sequence of the murine $\alpha$-cardiac actin gene (Sassoon *et al.* 1988) and pINT2fg, containing part of the murine *int-2* gene (Wilkinson *et al.* 1988), were also used as vectors for riboprobe synthesis.

Embryos (E3½, 5¼, 5¾, 6¼, 6½, 7, 7½, 8, 8½, and daily thereafter through E15½) were dissected from pregnant MF1 mice, fixed overnight at 4 °C in phosphate-buffered saline plus 4 % paraformaldehyde, and embedded in paraffin. E5¼ to E9½ embryos were left in their decidua. E3½ blastocysts were flushed from uteri, prefixed and loaded into dissected ampulae of pseudopregnant females before processing. Serial microtome sections (7–8 microns thick) were deparaffinized and hybridized essentially according to the procedure of Wilkinson (Wilkinson *et al.* 1987). The only modifications were in the content of the hybridization mix, which was prepared as previously described (Haub *et al.* 1990), and contained 3 nanograms probe in 0.2 ml per slide. After posthybridization RNAase treatment and washes (Wilkinson *et al.* 1987), slides were dipped in NTB2 emulsion (E. Kodak) diluted 1:1 with 2 % glycerol, and autoradiographed (14–20 days for $^{32}$P, 6 weeks for $^{35}$S). Exposed slides were developed in D19 (Kodak), stained with hematoxylin and eosin, and mounted with Permount (Fisher Scientific). Bright- and dark-field images were photographed from a Nikon Microphot-FXA microscope. All embryonic stages were exhaustively analyzed; multiple embryos were hybridized with both sense and antisense *Fgf-5* riboprobes, using a complete series of sections for each probe for E3½–E8½ embryos, and alternating groups of three sections for both probes with older, larger embryos. Anatomical assignments were made with the aid of several texts on embryonic anatomy (Gasser, 1975; Rugh, 1968; Theiler, 1989).

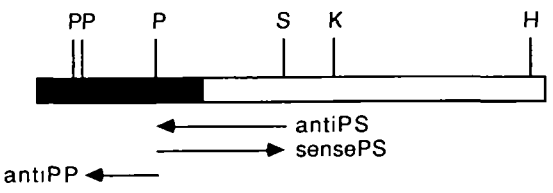


**Fig. 1.** Mouse *Fgf-5* cDNA and riboprobes. The bar represents the 2.2 kbp *Fgf-5* cDNA cloned from a mouse E11½ cDNA library. The coding region is filled in, while 3′ untranslated sequence is unfilled. *Pst*I (P), *Sac*I (S), *Hin*dIII (H), and *Kpn*I (K) cleavage sites are indicated. Riboprobes are shown with arrows. The *Pst*I–*Sac*I 450 bp region all derives from exon 3, and has been used previously to make antisense (antiPS) and sense (sensePS) ribroprobes (Haub *et al.* 1990). The more 5′ *Pst*I–*Pst*I cDNA fragment was used to make a corroborating riboprobe (antiPP).

### *Computer-aided three-dimensional modelling*

Camera-lucida drawings on transparencies were made from bright- and dark-field images of thirty hybridized sections spaced 96 microns apart across an E10½ embryo. The drawings were manually aligned, and then traced into a SunView computer using CARP software (Biographics, Inc.). Superimposed objects were 'built' from the contours of whole embryo, dorsal aorta and arches, primary head and cardinal trunk veins, *Fgf-5* signal in myotomes, and *Fgf-5* signal in somatic mesoderm, and visualized in various combinations for direct photography from the computer's screen.

## Results

In order to localize *Fgf-5* expression during embryogenesis, deparaffinized sections of prefixed mouse embryos at various stages of development were hybridized *in situ*, using radiolabelled antisense and sense *Fgf-5* RNA probes. Two different antisense probes, transcribed from nonoverlapping segments of *Fgf-5* cDNA (Fig. 1), detected identical profiles of gene expression. Hybridization to deparaffinized sections gives signals 3–4 fold weaker than to post-fixed, fresh frozen sections (our unpublished observations); in fact, our previous *in situ* analysis of *Fgf-5* expression in adult mouse brain required the use of fresh frozen sections to detect the very low abundance of *Fgf-5* RNA in this tissue (Haub *et al.* 1990). However, morphology in sections of fresh frozen embryos is very poor, mandating our use of paraffin-embedded material in these studies. With this technique, we have detected seven distinct sites of *Fgf-5* RNA expression in the mouse between embryonic days 3½ to 15½ post-conceptus[1].

### *Expression of* Fgf-5 *RNA in early embryogenesis*

Embryonic *Fgf-5* expression first occurs soon after uterine implantation. As can be seen in Fig. 2, there is no detectable expression in preimplantation blastocysts (panels E,F). *Fgf-5* RNA was detected in embryos at the next stage examined, E5¼ (panels A,B), while no signal was seen with the negative control (sense-strand) probe (panels C,D). The failure to detect *Fgf-5* expression in blastocysts (embryonic day 3½), cannot be attributed to the small size of the blastocyst; E5¼ expression was readily observed in tangential embryonic slices containing very few cells (data not shown). The postimplantation induction of expression is consist-

[1] We use standard nomenclature to define conception as midnight preceding the morning of vaginal plug detection. E3½=embryonic day 3½ postconceptus.

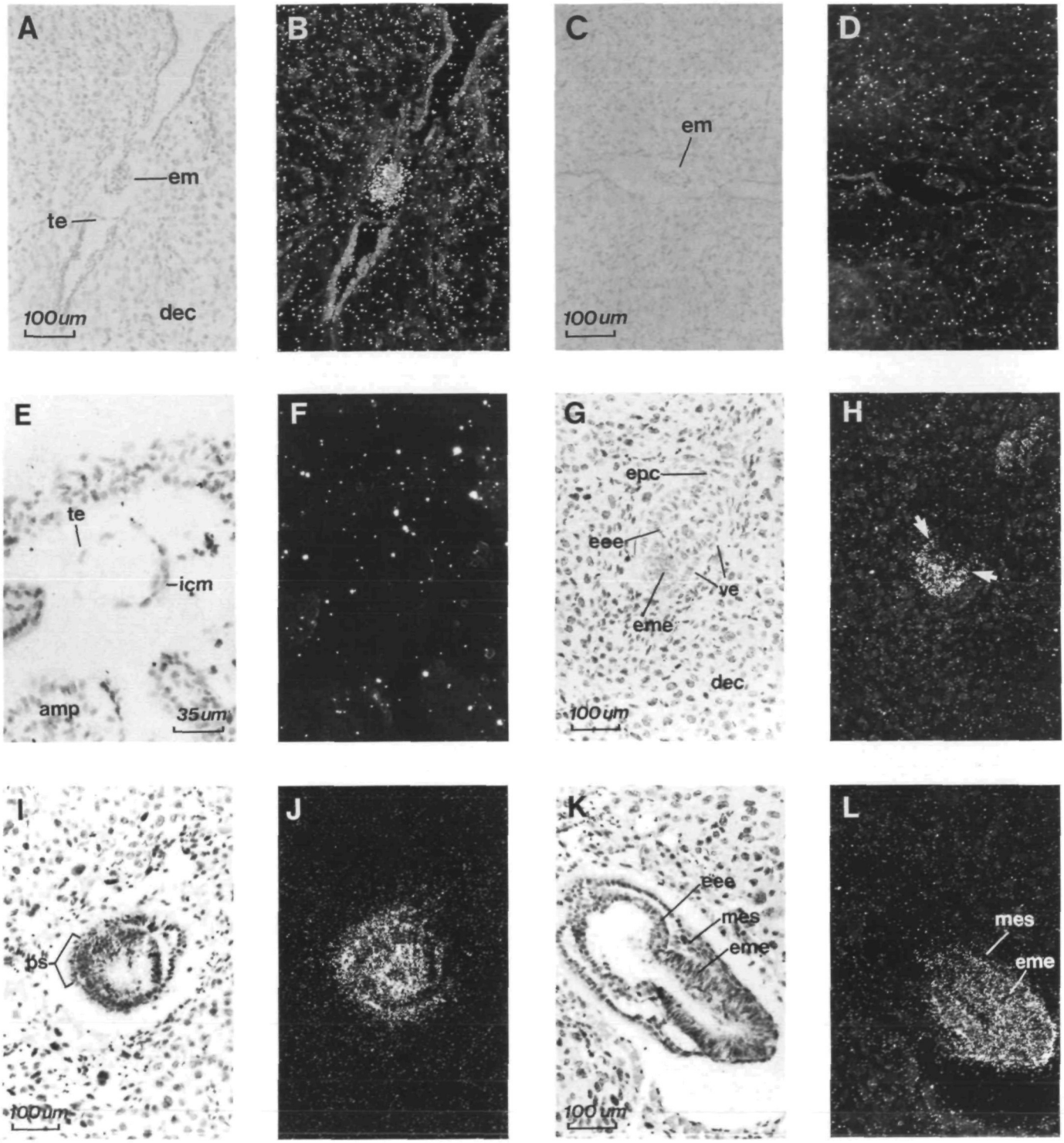


**Fig. 2.** *Fgf-5* RNA in early postimplantation embryos. AntiPS and sensePS *Fgf-5* $^{35}$S-riboprobes were hybridized to egg cylinders in decidua and to blastocysts manually loaded into ampulae of pseudopregnant mice. Dark-field imaging (panels B,D,F,H,J,K) makes exposed silver grains from NTB2 emulsion luminesce. Panels C,D used sensePS probe, while all other panels used the antiPS probe. Panels A,B and C,D, E5$\frac{1}{4}$ egg cylinder; E,F, E3$\frac{1}{2}$ blastocyst; G,H, E5$\frac{3}{4}$ egg cylinder, showing expression in embryonic ectoderm and adjacent visceral endoderm (arrows); I,J, cross-section through E7 egg cylinder; K,L, transverse section through E7 egg cylinder, showing expression in embryonic ectoderm, but not mesoderm. Embryo (em), deciduum, (dec), blastocyst inner cell mass (icm), trophectoderm (te), ampulla (amp), embryonic ectoderm (eme), extraembryonic ectoderm (eee), visceral endoderm (ve), ectoplacental cone (epc), mesoderm (mes), primitive streak (ps), microns (um).

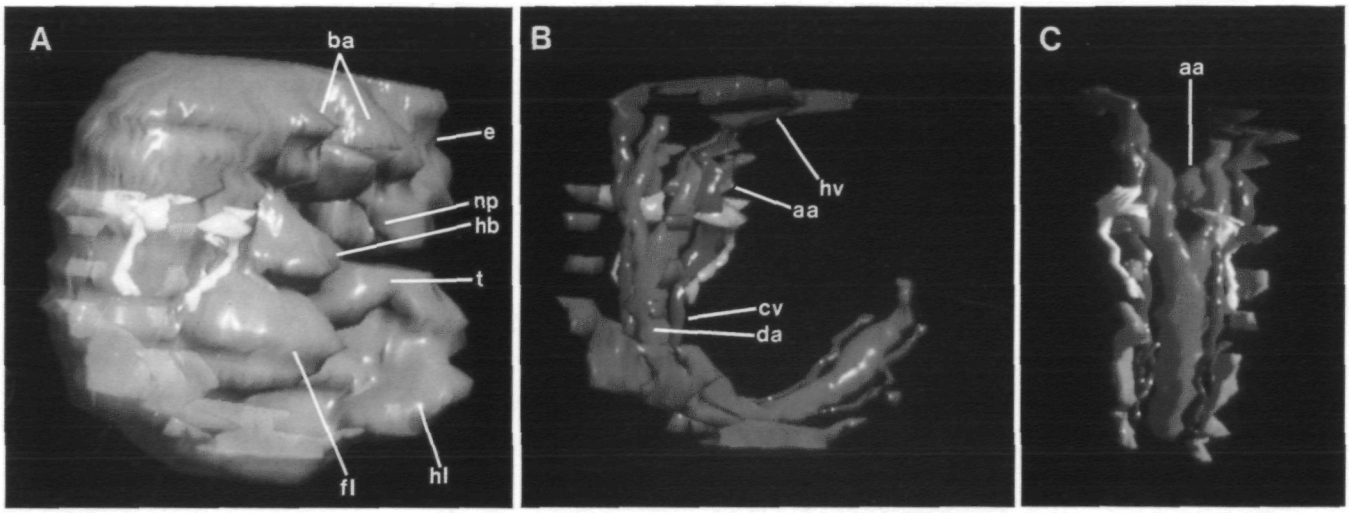


**Fig. 4.** Three-dimensional computer models of *Fgf-5* expression in an E10½ embryo. Thirty sections along an E10½ embryo hybridized with *Fgf-5* antiPS probe were used for modelling. For each section, a camera-lucida drawing of the embryo's contour, dorsal aorta and aortic arches, head vein and cardinal veins, and regions of *Fgf-5* expression in myotomes and somatic mesoderm was traced by computer 'mouse' into a SunView computer containing CARP (Biographics) software. The data was used to construct superimposed objects: embryo (tan), *Fgf-5* RNA in myotomes (pink), *Fgf-5* RNA in somatic mesoderm (yellow), arterial vasculature (red), and venous vasculature (blue). Panel A shows a dorsolateral view of the embryo rendered 'transparent' to reveal sites of *Fgf-5* expression. Panel B is the same view of *Fgf-5* expression along with vascular structures, with the embryo's exterior removed. Panel C is viewed dorsally. Eye (e), nasal pit (np), branchial arches (ba), forelimb bud (fl), hindlimb bud (hl), heart bulge (hb), tail (t), head vein (hv), cardinal vein (cv), dorsal aorta (da), aortic arches (aa). Sections from the top of the head (diencephalon) were not included in the analysis, giving the embryo a flat-top distortion. The use of one section per 96 microns (12 sections) and difficulties in section alignments also caused distortions and the artefactual fusion of some *Fgf-5*-positive myotomes.

ent with the observed rapid induction of *Fgf-5* mRNA levels when embryonal carcinoma cells or totipotent embryonic stem (ES) cells differentiate as embryoid bodies *in vitro* ((Hebert *et al.* 1990), and see below).

*Fgf-5* expression in E5¾ embryos is restricted to the embryonic ectoderm and adjacent visceral endoderm (Fig. 2, panels G,H). By contrast, extraembryonic ectoderm its flanking visceral endoderm and other extraembryonic tissues are negative. This same expression profile is evident through the onset of gastrulation at E6½ (data not shown). While expression in the embryonic ectoderm of the egg cylinder persists at E7, newly formed mesoderm is negative (panels K,L). A cross-section through the E7 egg cylinder illustrates *Fgf-5* RNA expression throughout the epiblast, without substantial lateral/medial or anterior/posterior variation (panels I,J). The E7½ embryo shows weaker *Fgf-5* RNA signals, and expression is undetectable in the E8 embryo.

The pattern of early embryonic expression for the *Fgf-5* gene contrasts with that for another gene in the FGF family, *int-2*. *int-2* is expressed in parietal extraembryonic endoderm and also in newly formed mesoderm leaving the primitive streak, commencing at E7½ (Wilkinson *et al.* 1988). By hybridizing adjacent E7½ embryo sections with *Fgf-5* and *int-2* antisense RNA probes, we have observed *Fgf-5* expression in embryonic ectoderm adjacent to *int-2* expression in mesoderm (data not shown).

### *Expression of* Fgf-5 *RNA in later embryogenesis*

Between embryonic days 9½ and 14½, six additional sites of *Fgf-5* expression are evident. Two of these sites are in derivatives of lateral mesoderm, two others are skeletal muscle precursors derived from paraxial mesoderm, and the other two sites are limb mesenchyme and a cranial ganglion (see below). On embryonic day 15½, no sites of *Fgf-5* expression are identifiable *in situ*. Since *Fgf-5* RNA can still be detected by northern blot analysis at this developmental stage (Hebert *et al.* 1990), our *in situ* hybridization assays are failing to detect very low levels of expression in unidentified tissues. We estimate such expression to be <10 copies mRNA/cell (discussed later).

### Fgf-5 *RNA in lateral mesoderm*

On embryonic day 9½, the *Fgf-5* gene is expressed in one small region of splanchnic mesoderm ventral to the portion of the foregut bearing the hepatic bud (Fig. 3, panels A–C). Expression in this mesenchyme is less readily detectable on E10½ (data not shown), and undetectable thereafter. The onset of expression is approximately coincident with that of rapid liver growth, which proceeds by the invasion of hepatic cords from the hepatic bud into the underlying mesenchyme. Whether the apparent fall-off of splanchnic mesodermal *Fgf-5* expression from E9½ to E10½ represents down-regulation or merely the dilution of signal due to mesenchyme thinning and intermingling with hepatic cells cannot be ascertained.

*Fgf-5* RNA is expressed in a region of somatic mesoderm between E10½ and E12½. On embryonic day 10½, this region extends rostrocaudally from the level of the newly formed sixth aortic arch to approximately the level of the liver primordium. Fig. 3 shows this expression in a transverse section through a E10½ embryo (panels F,G) and a parasagittal section through a E11½ embryo (panels H,I). *Fgf-5* expression also occurs in myotomes at these times (see below). The somatic mesoderm signal is readily distinguished from that of skeletal muscle precursors by hybridization of adjacent sections with a probe for α-cardiac actin mRNA (Sassoon *et al.* 1988), which is expressed in striated muscle cells and their precursors. This is illustrated in Fig. 3, panel J, where the actin probe detects myotomes and cardiac muscle in the E11½ embryo, but does not hybridize to somatic mesoderm.

In order to illustrate the overall region of somatic mesoderm expressing *Fgf-5* RNA in the E10½ embryo and the proximity of this region to vascular structures, the data in thirty transverse sections spaced 96 microns apart were used for three-dimensional computer modelling. CARP software (Computer-Aided Reconstruction Package, Biographics Inc.) was used to generate models of the entire embryo, dorsal aorta and aortic arches, primary head veins and cardinal trunk veins, and sites of somatic mesoderm and myotome *Fgf-5* expression (Fig. 4). The broad anterior regions of *Fgf-5*-positive somatic mesoderm (panels A–C) lie both lateral and just caudal to the newly formed sixth aortic arch. It is worth noting that this approximate region of expression sees the enlargement of the sixth arch and the emergence of a caudally projecting vascular branch (the future pulmonary artery) during the ensuing 36 h of development. The caudal 'tails' of expression in the E10½ embryo run adjacent to the paired cardinal veins (panels B,C).

### Fgf-5 *expression in skeletal muscle precursor cells*

Skeletal muscles of the trunk and limbs are descendants of the somites, which arise by segmentation of paraxial mesoderm in an anterior-to-posterior sequence beginning at E8¼. Each maturation phase of anterior somites precedes that of posterior ones owing to their different times of birth. The precursor cells for limb muscle emigrate from the newly formed myotome derivative of the somite and enter limb buds shortly after their formation on E9½ (forelimb) and E10 (hindlimb) (Sassoon *et al.* 1989). The trunk muscle precursor cells remain in the segmented myotomes and commence migration on E10½ to E11½.

*Fgf-5* RNA is expressed in myotomes starting on E10½ (Fig. 3, panels D–G). This induction occurs later than the morphological appearance of myotomes (E8½) and their expression of α-cardiac actin mRNA (E8½–E9½) ((Sassoon *et al.* 1989), and our observations). On embryonic day 10½, only myotomes anterior to the middle of the hindlimb bud are *Fgf-5* positive, as shown in the 3-D model (Fig. 4, panel A). More caudal myotomes also express *Fgf-5* RNA a day later, reflecting their delayed development, but tail region myotomes never express *Fgf-5* (data not shown).

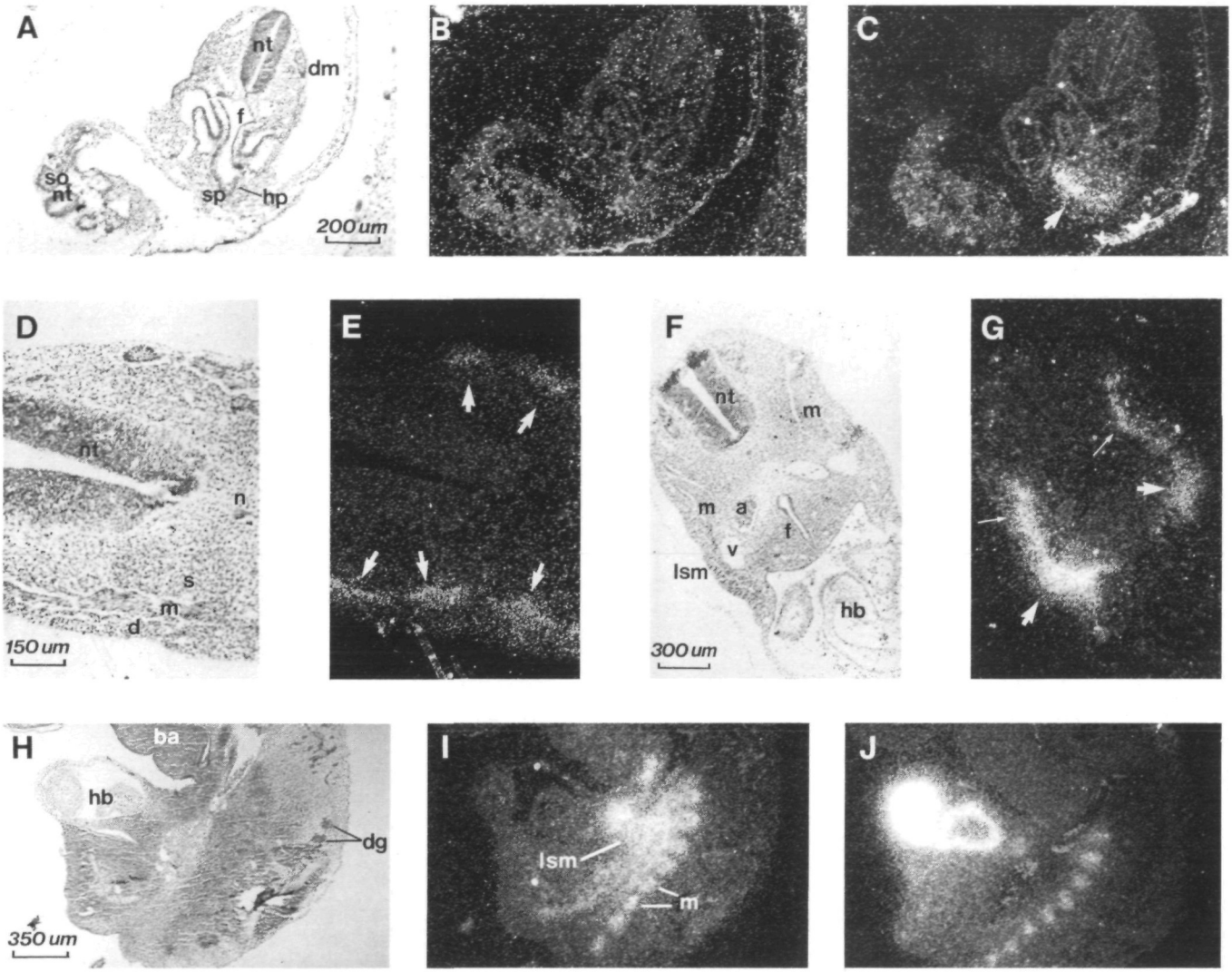


**Fig. 3.** *Fgf-5* RNA in lateral mesoderm and myotomes. Hybridizations were with antiPS *Fgf-5*, sensePS *Fgf-5*, and α-cardiac actin $^{32}$P-riboprobes. Panels B,C,E,G,I,J are dark field images. Panels A–C, adjacent E9½ sections hybridized with sensePS (A,B) or antiPS (C) with *Fgf-5*-positive lateral splanchnic mesoderm (arrow); panels D,E, E10½ longitudinal section through rostral somites, antiPS probe with *Fgf-5*-positive myotomes (arrows); panels F,G, E10½ transverse section through rostral tip of heart bulge, antiPS probe, with *Fgf-5*-positive myotomes (thin arrows) and lateral somatic mesoderm (thick arrows); panels H–J, adjacent E11½ parasagittal sections hybridized with antiPS (H,I) and α-cardiac actin (J) probes. Hepatic bud (hp), foregut (f), lateral splanchnic mesoderm (sp), neural tube (nt), notocord (n), dermatome (d), myotome (m), dermamyotome (dm), somite (so), sclerotome (s), dorsal aorta (a), cardinal vein (v), heart bulge (hb), lateral somatic mesoderm (lsm), branchial arch (ba), dorsal root ganglia (dg).

Myotomal cells continue to express *Fgf-5* RNA on E11½ (Fig. 3, panels H–J) and E12½ (data not shown) during their ventral and lateral migration. Expression in trunk muscle precursor cells is barely evident in E13½ embryos and is undetectable by E14½. By contrast to trunk muscle differentation, precursors of limb muscles, identifiable by α-cardiac actin RNA expression (see below), do not express *Fgf-5* RNA at any stage in their development.

Cranial skeletal muscles (tongue, mastication, extrinsic ocular and facial) all derive from paraxial mesoderm in birds (Noden, 1988), and similar origins in mammals are suspected. A prominent site of *Fgf-5* RNA expression in the head of the E13½ embryo (Fig. 5, panel F) corresponds to the mastication muscle precursor cells. Hybridization of a nearly adjacent section with the α-cardiac actin probe (Fig. 5, panels D,E) reveals expression in mastication muscles as well as in the extrinsic ocular muscles. Facial and tongue muscle lineages, as recognized by α-cardiac actin hybridization, are also *Fgf-5* negative (data not shown). The strong *Fgf-5* mastication muscle signal persists on E14½, but is completely absent 24 h later (data not shown). This site of *Fgf-5* RNA expression originates on embryonic day 11½ as bilateral patches, each situated near the juncture of the maxillary process and the mandibular arch (Fig. 5, panels A,B). Curiously, α-cardiac actin RNA expression is very weak at this site

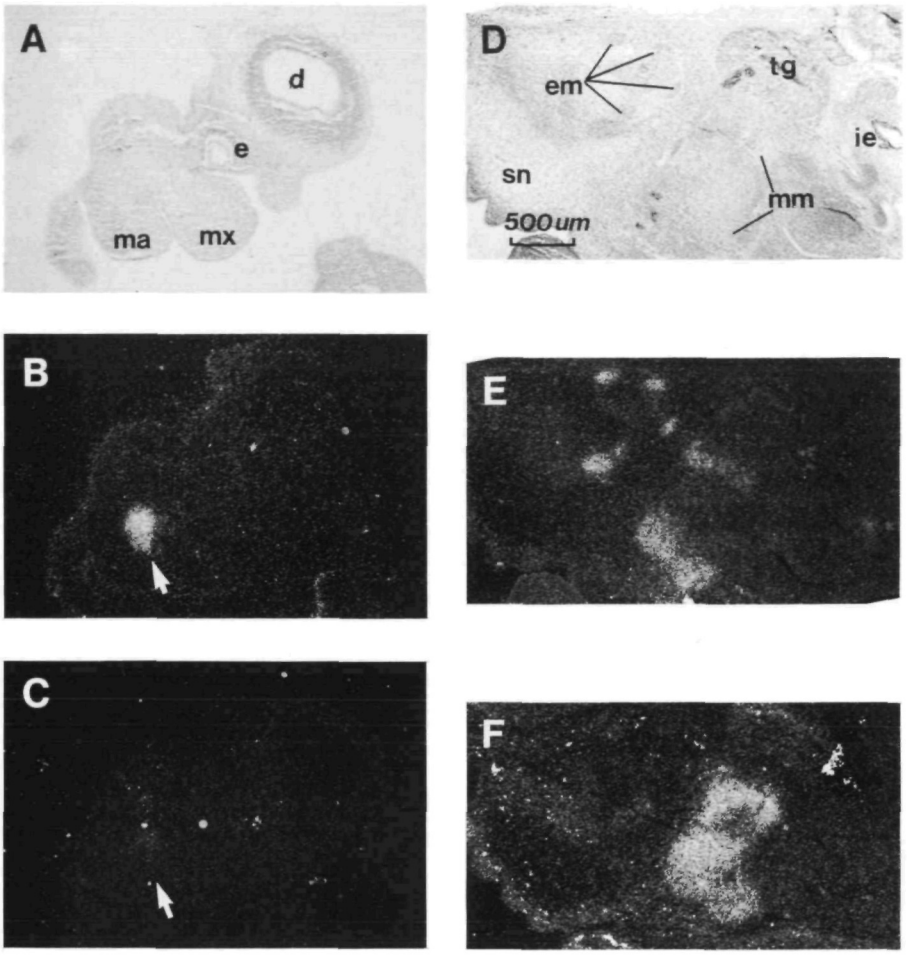


**Fig. 5.** *Fgf-5* RNA in mastication muscle. Sections were hybridized with *Fgf-5* antiPS and α-cardiac actin $^{32}$P-riboprobes. Panels B,C,E,F are dark-field images. Adjacent E11½ tangential sagittal sections through the head hybridized with antiPS (panels A,B) and α-cardiac actin (C) probes. Arrows denote strong *Fgf-5* and very weak α-cardiac actin signals. Nearly adjacent E13½ parasaggital sections through the head hybridized with α-cardiac actin (panels D,E) and antiPS (F) probes. While the actin probe detects extrinsic ocular and mastication muscles, the *Fgf-5* probe detects only the latter. Maxillary process (mx), mandibular arch (ma), eye (e), diencephalon (d), snout (sn), extrinsic eye muscles (em), mastication muscles (mm), trigeminal ganglion (tg), inner ear (ie).

(Fig. 5, panel C), and only becomes prominent on E12½ (data not shown).

These cranial expression data are open to radically different interpretations. Mastication muscle precursor cells may strongly express *Fgf-5* RNA in advance of substantial α-cardiac actin RNA expression. This would represent the opposite temporal order of gene expression from that which occurs in myotomes. Alternatively, the cranial *Fgf-5* RNA expression at E11½ may be in mesenchyme of neural crest or lateral mesoderm origin which neighbors or is intermingled with muscle cell precursors.

### Fgf-5 *RNA in developing limbs*

*Fgf-5* RNA has been detected in developing limbs from embryonic days 12½ through 14½. Expression is limited to a patch of cells near the base of each limb, and while expression is readily detected in hindlimbs, it is far less evident in forelimbs. Panels A and B of Fig. 6 shows the expression patch in a transverse section through the E12½ hindlimb. In the E13½ embryo, parasagittal sections, which effectively represent cross-sections through the base of the limb, show that the mesenchymal region of *Fgf-5* expression (panel E) is ventral to the femur (panel D), which is undergoing chondrification. The expression site is distinct from the various developing muscle groups, which are visualized in adjacent sections by their expression of α-cardiac actin RNA (panel E). The tracing in panel G illustrates the spatial relationship of *Fgf-5* positive mesenchyme to developing muscle and cartilage. The weaker *Fgf-5* RNA signal in forelimbs is positioned similarly to that in hindlimbs (data not shown).

### Fgf-5 *RNA in the acoustic ganglion*

*Fgf-5* RNA has been detected in the acoustic branch of the eighth cranial ganglion within the inner ear on embryonic days 12½ through 14½ (Fig. 6, panels G–J). All other cranial ganglia lack detectable *Fgf-5* RNA, including the vestibular branch of the eighth ganglion (Fig. 6, panels G,H) and the trigeminal fifth ganglion (Fig. 5, panels D,F). The cochlea is another developmental site where *Fgf-5* and *int-2* RNAs are expressed in neighboring cells. *int-2* is expressed in portions of the cochlear sensory epithelium and underlying mesenchyme (Wilkinson *et al.* 1989), which are innervated by projections from acoustical neurons.

The seven sites of *Fgf-5* embryonic expression are catalogued in Table 1.

### *Levels of* Fgf-5 *RNA in the egg cylinder*

The measurement of intracellular *Fgf-5* RNA concentration is only possible in tissues where dissection allows isolation of expressing cells to a known degree of purity. The one site amenable to RNA quantitation is the

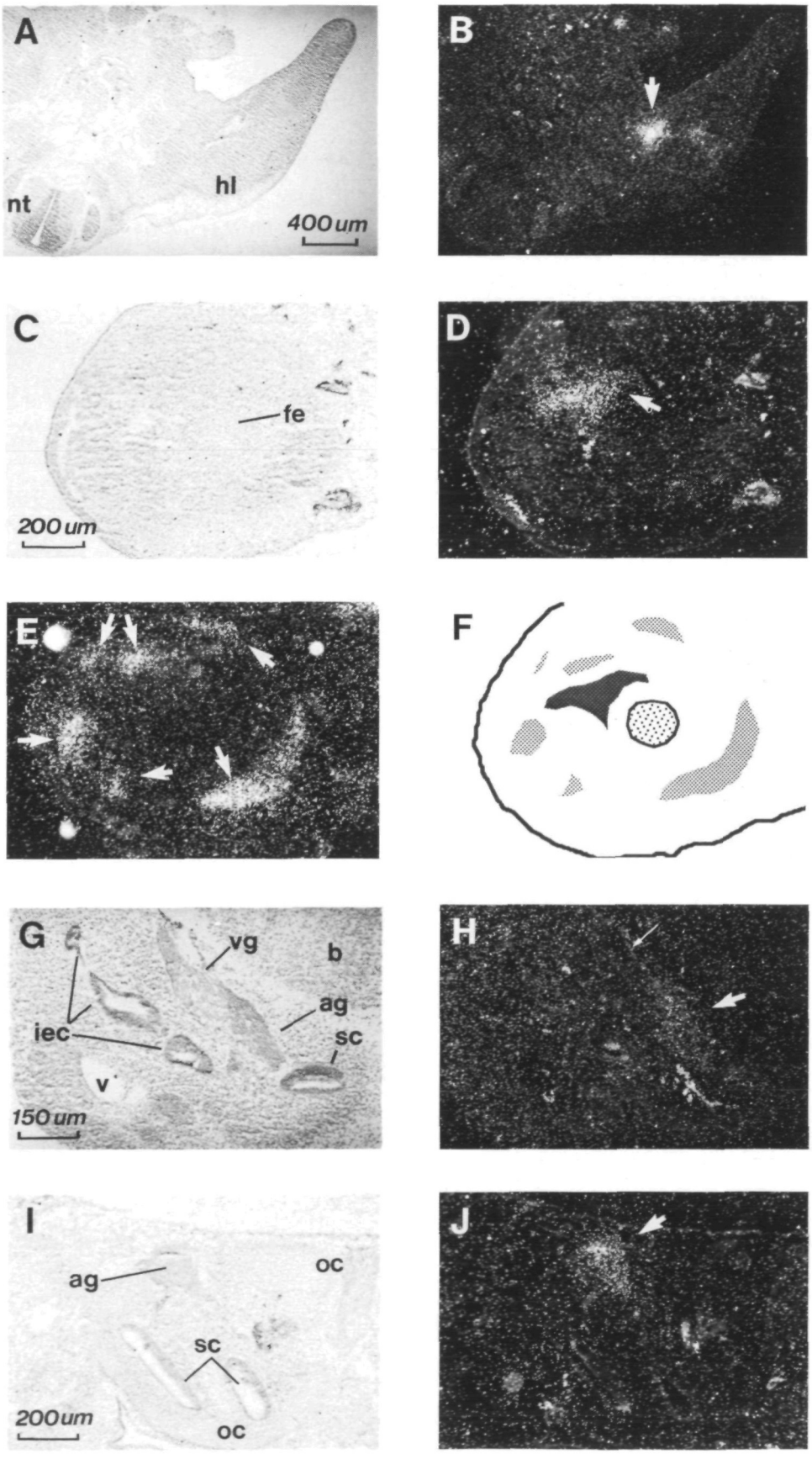


**Fig. 6.** *Fgf-5* RNA in hindlimb and acoustic ganglion. Sections were hybridized with *Fgf-5* antiPS, antiPP, and α-cardiac actin $^{32}$P-riboprobes. Panels B,D,E,H,J are dark-field images. Panels A,B, hybridization of *Fgf-5* antiPP probe to E12½ transverse section through hindlimb, showing positive patch near base of limb (arrow). Panels C–E, adjacent E13½ parasagittal sections through base of hindlimb hybridized with *Fgf-5* antiPS (C,D) and α-cardiac actin (E) probes. Arrows in D and E denote *Fgf-5*-positive mesenchyme and α-cardiac actin-positive limb muscle groups, respectively. Panel F, E13½ hindlimb schematic derived by tracings from panels C–E, showing femur cartilage (spotted), α-cardiac actin-positive muscle precursors (light shaded), and *Fgf-5*-positive mesenchyme (dark shaded). Panels G,H, longitudinal section through head of E12½ embryo hybridized with *Fgf-5* antiPP probe, showing expression in acoustical branch of eighth ganglion (bold arrow), but not in more lateral vestibular branch (thin arrow). Panels I,J, parasagittal section through head of E14½ embryo hybridized with antiPS probe. Arrow denotes expression in acoustic ganglion. Hindlimb (hl), neural tube (nt), femur (fe), acoustic ganglion (ag), vestibular ganglion (vg), brain (b), spiral canal (sc), other canals of inner ear (iec), otic capsule (oc), head vein (v).

**Table 1.** *Embryonic sites of FGF-5 gene expression*

| Expression site | Days of gestation | Comments |
|---|---|---|
| Epiblast and surrounding visceral endoderm | 5.3–7.5 | Negative in E3.5 blastocyst; Negative in egg cylinder mesoderm and extraembryonic tissues |
| Lateral splanchnic mesoderm adjacent to hepatic bud | 9.5–10.5 | Negative in all other splanchnic mesoderm |
| Region of lateral somatic mesoderm | 10.5–12.5 | Prominent expression near arterial vessels |
| Myotomal muscle lineages | 10.5–12.5 weak at 13.5 | Negative in limb muscle lineages and tail myotomes |
| Mastication muscle lineage | 11.5–14.5 | Negative in other cranial skeletal muscles E11.5 expression in myoblasts or mesenchyme |
| Mesenchyme near base of limb (hind>fore) | 12.5–14.5 | Negative in limb muscle and cartilage |
| Acoustic ganglion | 12.5–14.5 | Negative in other cranial ganglia |

postimplantation egg cylinder. On embryonic day $6\frac{3}{4}$–7, embryonic ectoderm accounts for ~70% of the cells in the embryonic compartment (embryonic ectoderm, mesoderm, flanking visceral endoderm) (Snow, 1977), and this compartment is larger than the extraembryonic compartment of the egg cylinder. Hence, the embryonic ectodermal cells expressing *Fgf-5* RNA constitutes 40–50% of the cells in the egg cylinder.

Thirty egg cylinders (embryonic day $6\frac{3}{4}$–7) were dissected from decidua, teased free of ectoplacental cone tissue and dissolved in guanidinium isothiocyanate for the isolation of RNA. An aliquot of the RNA was analyzed by northern blotting for GAPDH mRNA, a constitutively expressed message, as compared to GAPDH mRNA levels in known amounts of ES cell RNA. The analysis demonstrated a recovery of one microgram total RNA from the egg cylinders (data not shown). The egg cylinder RNA was then analyzed for *Fgf-5* mRNA by northern blot hybridization, and the signal compared to those obtained for several quantities of *Fgf-5* cDNA. As shown in Fig. 7, one microgram RNA from 30 egg cylinders gave a 2.9 kb *Fgf-5* RNA signal (lane e) comparable to 2 picograms 2.2 kb *Fgf-5* cDNA (lane b). From this, we calculate that *Fgf-5* mRNA represents $2.5\times10^{-6}$ of the total egg cylinder RNA. Since the embryonic compartment of each E$6\frac{3}{4}$–7 egg cylinder contains ~3000 cells (Snow, 1977), the estimated level of egg cylinder *Fgf-5* expression is 30–40 copies/embryonic ectodermal cell.

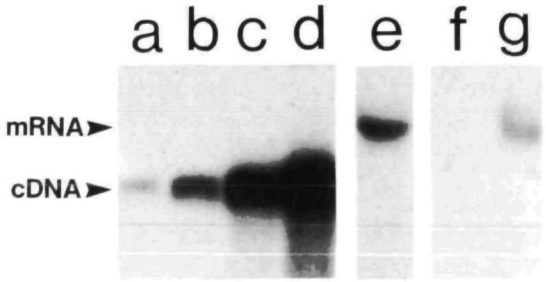


**Fig. 7.** Northern blot quantitation of *Fgf-5* RNA in egg cylinders. Total RNA (one microgram) from E$6\frac{3}{4}$–7 egg cylinders (lane e), undifferentiated ES cells (lane f), and ES cell-derived embryoid bodies (three days in suspension) (lane g) were analyzed by formaldehyde–agarose gel electrophoresis and filter blot hybridization, using murine *Fgf-5* $^{32}$P-labelled cDNA as probe. Denatured 2.2 kbp murine *Fgf-5* cDNA (0.5 pg, lane a; 2 pg, b; 10 pg, c; 50 pg, d) was also analyzed to allow quantitation of *Fgf-5* RNA. The hybridization signal from 1 $\mu$g egg cylinder RNA (lane e) equalled that from 2 pg *Fgf-5* cDNA (lane b).

The *Fgf-5* RNA expression level in the egg cylinder (lane e) is similar to that in ES cells allowed to differentiate into simple embryoid bodies following three days in suspension (lane g), and is dramatically higher than the level expressed in undifferentiated ES cells, which is undetectable at the exposure length shown (lane f). These simple embryoid bodies have morphological features comparable to the egg cylinder prior to gastrulation (Martin *et al.* 1977). Hence, the induction of *Fgf-5* expression in embryoid bodies quantitatively and temporally parallels the *Fgf-5* gene's *in vivo* induction postimplantation.

The intensity of the *Fgf-5 in situ* hybridization signal in egg cylinders was consistently equal to or stronger than those seen locally at the later sites of *Fgf-5* gene expression. We estimate local expression in later embryogenesis to be at 10–30 copies mRNA/cell. Due to the constraints of signal *versus* background, we do not feel that our assay conditions could detect <10 copies RNA/cell. Hence, sites of very weak expression could be missed in our analysis. This presumably explains our failure to define the sites of *Fgf-5* expression in the E$15\frac{1}{2}$ day embryo. Additionally, our preliminary *in situ* analysis of E$13\frac{1}{2}$ embryos, using fresh frozen tissue for higher sensitivity, has revealed weak sites of *Fgf-5* expression (dorsal root ganglia, myenteric ganglia) in addition to the more prominent hindlimb, mastication muscle and acoustic ganglion signals described earlier.

## Discussion

Embryonic expression of the *Fgf-5* gene is regulated as a function of time, tissue type and position within tissue. This lattermost characteristic has defined subdivisions of splanchnic mesoderm, somatic mesoderm and

limb mesenchyme that were not morphologically evident nor previously appreciated by other molecular criteria. The spatial restriction of expression may, in part, be governed by combinations of transcription factors, such as homeobox proteins, which themselves are expressed within spatial boundaries. For example, the expression boundaries of various homeobox genes in vertebrate limbs define a 'grid' along both anterior–posterior and proximal–distal axes (Smith *et al.* 1989), and this grid may help dictate *Fgf-5* expression in limb mesenchyme. Another manifestation of spatially restricted expression is the presence of *Fgf-5* RNA in some skeletal muscle groups and cranial ganglia, but not in others.

The structurally related *int-2* gene is also expressed in a complex spatiotemporal pattern, although the sites of expression differ from those for the *Fgf-5* gene (Wilkinson *et al.* 1989; Wilkinson *et al.* 1988). At certain stages in development, *Fgf-5* and *int-2* are expressed in close proximity: *Fgf-5* in visceral endoderm *versus int-2* in parietal endoderm, *Fgf-5* in E7½ embryonic ectoderm *versus int-2* in E7½ embryonic mesoderm, and *Fgf-5* in acoustic ganglion *versus int-2* in cochlear sensory epithelium. Since both of these growth factors are secreted proteins (Bates *et al.* 1991; Dixon *et al.* 1989), we suspect that FGF receptors expressed in these regions differentially react with or respond to these two FGFs. While the known spectra of *in vitro* biological activities are similar among FGFs, there are contrasts (Finch *et al.* 1989; Lipton *et al.* 1988; Valles *et al.* 1990) which are presumably mediated by differences in ligand–receptor interactions.

FGF-5 is likely to mediate a diverse set of events during embryogenesis. The *Fgf-5* expression profile along with known biological effects of other FGFs in *in vitro* and *in vivo* assays allow for speculation regarding FGF-5's native functions. Such conjecture merely serves as a guide for further studies.

Uterine implantation of the blastocyst is followed by rapid growth of the egg cylinder and rapid growth of the uterine deciduum. *Fgf-5* expressed in embryonic ectoderm postimplantation could serve as an autocrine or paracrine factor to mediate these growth events. Several FGFs have been shown to possess mesoderm-inducing activity when assayed on cultures of amphibian animal cap ectoderm (Kimelman and Kirschner, 1987; Paterno *et al.* 1989; Slack *et al.* 1987). The expression of *Fgf-5* RNA at the onset of mouse gastrulation suggests that this growth factor may contribute to mesoderm formation, although two facts argue against a direct role for FGF-5 in this process: (1) the onset of gene expression (≤E5¼) far precedes the start of gastrulation (E6½), and (2) *Fgf-5* RNA is not spatially restricted within the embryonic ectoderm. Future localization of *Fgf-5* protein and receptors in the developing egg cylinder is of obvious importance.

Acidic and basic fibroblast growth factors are mitogenic for vascular endothelial cells *in vitro* and are angiogenic when applied to tissues *in vivo* (Burgess and Maciag, 1989). FGF-5 is most likely an endothelial cell mitogen, since conditioned medium containing secreted FGF-5 will stimulate endothelial cell growth (Zhan *et al.* 1988). FGF-5 might act as an angiogenic factor in lateral mesoderm, which becomes more highly vascularized than dorsal mesoderm (Le Douarin, 1975; Sherer, 1975). In splanchnic mesoderm, local *Fgf-5* expression might promote vascularization required for the induction of neighboring hepatic cord proliferation (Sherer, 1975). In somatic mesoderm, local *Fgf-5* expression could contribute to the ongoing remodelling of the arterial vasculature (Rugh, 1968).

FGFs have well-documented effects upon the differentiation of skeletal muscle progenitor cells. Fibroblast growth factors can inhibit the terminal differentiation of myoblasts, as monitored by biochemical markers and by myotube formation (Lathrop *et al.* 1985; Seed and Hauschka, 1988). *Fgf-5* expression commences in myotomes on E10½ well after their formation (E8½) and commitment to muscle lineage, as gauged by the onset of a-cardiac actin (E8½–9½) and MyoD (E9½) gene expression (Sassoon *et al.* 1989). *Fgf-5* expression diminishes by E13½, before the first appearance of myotubes on E15 (Rugh, 1968). FGF-5 could inhibit the terminal differentiation of myotomal myoblasts during their migration through the trunk. Limb muscle development differs from that of trunk muscle by several molecular criteria. The onset of α-cardiac actin and MyoD expression in limb muscle precursors occurs later in embryogenesis (Sassoon *et al.* 1989), although appearance of myofibrils occurs at similar times for limb and trunk muscle (Rugh, 1968); i.e. the later stages of muscle differentiation transpire within a more compressed time frame in limb *versus* trunk. A lack of *Fgf-5* expression in limb muscle myoblasts might account for their more rapid terminal differentiation.

*In vitro* culture of dissociated chicken limb bud cells has revealed an FGF-dependent subcomponent of myoblasts which require treatment with basic FGF in order ultimately to form colonies of terminally differentiated muscle (Seed and Hauschka, 1988). It is possible that E12½–14½ *Fgf-5* expression in limb mesenchyme acts to induce the development of FGF-dependent limb myoblasts. Furthermore, if the mandibular site of E11½ *Fgf-5* expression consists of mesenchymal as opposed to myoblastic cells, such expression could act to induce local myoblasts to develop into the mastication muscle groups.

Several lines of experimentation are required to elucidate FGF-5's roles in embryogenesis. FGF's receptors and their sites of expression need to be identified. Alternatively spliced transcripts of the FLG and BEK genes encode a family of related FGF receptors (reviewed in (Goldfarb, 1990)), but their affinities toward FGF-5 await characterization. A more precise cellular assignment of *Fgf-5* expression is clearly desirable, particularly as it relates to mesenchymal *versus* myoblastic gene expression in the mandibular region. Transgenes linking an enzymatic reporter to *Fgf-5* transcriptional regulatory elements may provide such insights. Lastly, the use of *in vivo* gene targetting to disrupt FGF-5 production partially or completely may generate informative embryonic phenotypes.

We thank Beverly Drucker for help in several experiments, and Matthew Buttrick for assisting in paraffin embedding and sectioning. We are most grateful to David Sassoon (Boston University) and to Godon Peters (Imperial Cancer Research Fund, London) for $\alpha$-cardiac actin and *int-2* clones, respectively, to Elizabeth Robertson for providing ES cells, to Francoise Poirier for instruction in egg cylinder dissection, to James Lee for help with blastocyst preparation, to Connie Cepko (Harvard Medical School) for access to her SunView/CARP 3-D imaging system, and to Lisa Jepeol and Elizabeth Ryder for instruction in its use. We also thank Vassilus Pachnis, Jane Dodd, Taube Rothman, David Sassoon, Elizabeth Taparowsky (Purdue University) and Cliff Tabin (Harvard Medical School) for helpful discussions. This work was supported by PHS research grant CA48054. O.H. is supported by NIH Training Grant DK07328.

## References

ANDERSON, K. J., DAM, D., LEE, S. AND COTMAN, C. W. (1988). Basic fibroblast growth factor prevents death of lesioned cholinergic neurons *in vivo*. *Nature* **332**, 360–361.

BATES, B., HARDIN, J., ZHAN, X., DRICKAMER, K. AND GOLDFARB, M. (1991). Biosynthesis of human fibroblast growth factor-5. *Molec. cell. Biol.* **11**, 1840–1845.

BIRREN, S. J. AND ANDERSON, D. J. (1990). A v-myc immortalized sympathoadrenal progenitor cell line in which neuronal differentiation is initiated by FGF but not NGF. *Neuron* **4**, 189–201.

BURGESS, W. H. AND MACIAG, T. (1989). The heparin-binding (fibroblast) growth factor family of proteins. *A. Rev. Biochem.* **58**, 575–606.

CHIRGWIN, J. M., PRYZBYLA, A. E., MACDONALD, R. J. AND RUTTER, W. J. (1979). Isolation of biologically active ribonucleic acid from sources enriched in ribonuclease. *Biochemistry* **18**, 5294–5299.

DIXON, M., DEED, R., ACLAND, P., MOORE, R., WHYTE, A., PETERS, G. AND DICKSON, C. (1989). Detection and characterization of the fibroblast growth factor-related oncoprotein INT-2. *Molec. cell. Biol.* **9**, 4896–4902.

FEINBERG, A. AND VOGELSTEIN, B. (1983). A technique for radiolabelling DNA restriction endonuclease fragments to high specific activity. *Anal. Biochem.* **132**, 6–13.

FINCH, P. W., RUBIN, J. S., MIKI, T., RON, D. AND AARONSON, S. A. (1989). Human KGF is FGF-related with properties of a paracrine effector of epithelial cell growth. *Science* **245**, 752–755.

FOLKMAN, J. AND KLAGSBRUN, M. (1987). Angiogenic factors. *Science* **235**, 442–447.

FORT, P., MARTY, L., PIECHACZYK, M., SABROUTY, S. E., DANI, C., JEANTEUR, P. AND BLANCHARD, J. M. (1985). Various rat tissues express only one major mRNA species from the glyceraldehyde-3-phosphate dehydrogenase multigenic family. *Nucl. Acids Res.* **13**, 1431–1442.

GASSER, R. M. (1975). *Atlas of Human Embryos*. Harper and Row, Hagerstown.

GOLDFARB, M. (1990). The fibroblast growth factor family. *Cell Growth Differ.* **1**, 439–445.

HATTEN, M. E., LYNCH, M., RYDEL, R. E., SANCHEZ, J., JOSEPH-SILVERSTEIN, J., MOSCATELLI, D. AND RIFKIN, D. B. (1988). *In vitro* neurite extension by granule neurons is dependent upon astroglial-derived fibroblast growth factor. *Devl Biol.* **125**, 280–289.

HAUB, O., DRUCKER, B. AND GOLDFARB, M. (1990). Expression of murine fibroblast growth factor-5 in the adult central nervous system. *Proc. natn. Acad. Sci. U.S.A.* **87**, 8022–8026.

HEBERT, J. M., BASILICO, C., GOLDFARB, M., HAUB, O. AND MARTIN, G. R. (1990). Isolation of cDNAs encoding four mouse FGF family members and characterization of their expression during embryogenesis. *Devl Biol.* **138**, 454–463.

KIMELMAN, D. AND KIRSCHNER, M. (1987). Synergistic induction of mesoderm by FGF and TGF-$\beta$ and the identification of an mRNA coding for FGF in the early *Xenopus* embryo. *Cell* **51**, 869–877.

LATHROP, B., OLSON, E. AND GLASER, L. (1985). Control by fibroblast growth factor of differentiation in the BC3H1 muscle cell line. *J. Cell Biol.* **100**, 1540–1547.

LE DOUARIN, N. M. (1975). An experimental analysis of liver development. *Med. Biol.* **53**, 427–455.

LIPTON, S. A., WAGNER, J. A., MADISON, R. D. AND D'AMORE, P. A. (1988). Acidic fibroblast growth factor enhances regeneration of processes by postnatal mammalian retinal ganglion cells in culture. *Proc. natn. Acad. Sci U.S.A.* **85**, 2388–2392.

MARTIN, G. R. AND EVANS, M. J. (1975). Multiple differentiation of clonal teratocarcinoma stem cells following embryoid body formation *in vitro*. *Cell* **6**, 467–474.

MARTIN, G. R., WILEY, L. M. AND DAMJANOV, I. (1977). The development of cystic embryoid bodies *in vitro* from clonal teratocarcinoma stem cells. *Devl Biol.* **61**, 230–244.

MELTON, D. A., KRIEG, P. A., REBAGLIATI, M. R., MANIATIS, T., ZINN, K. AND GREEN, M. R. (1984). Efficient *in vitro* synthesis of biologically active RNA and RNA hybridization probes from plasmids containing a bacteriophage SP6 promoter. *Nucleic Acid Res.* **12**, 7035–7056.

MORRISON, R. S., SHARMA, A., DE VELLIS, J. AND BRADSHAW, R. A. (1986). Basic fibroblast growth factor suppports the survival of cerebral cortical neurons in primary culture. *Proc. natn. Acad. Sci. U.S.A.* **83**, 7537–7541.

NODEN, D. (1988). Interactions and fates of avian craniofacial mesenchyme. *Development* **103 Supplement**, 121–140.

PATERNO, G. D., GILLESPIE, L. L., DIXON, M. S., SLACK, J. M. W. AND HEATH, J. K. (1989). Mesoderm-inducing properties of INT-2 and kFGF: two oncogene-encoded growth factors related to FGF. *Development* **106**, 79–83.

RUGH, R. (1968). *The Mouse: its Reproduction and Development*. Burgess, Minneapolis.

SASSOON, D., LYONS, G., WRIGHT, W. E., LIN, V., LASSAR, A., WEINTRAUB, H. AND BUCKINGHAM, M. (1989). Expression of two myogenic regulatory factors myogenin and MyoD1 during mouse embryogenesis. *Nature* **341**, 303–307.

SASSOON, D. A., GARNER, I. AND BUCKINGHAM, M. (1988). Transcripts of $\alpha$-cardiac and $\alpha$-skeletal actins are early markers for myogenesis in the mouse embryo. *Development* **104**, 155–164.

SEED, J. AND HAUSCHKA, S. D. (1988). Clonal analysis of vertebrate myogenesis VIII. Fibroblast growth factor (FGF)-dependent and FGF-independent muscle colony types during chick wing development. *Devl Biol.* **128**, 40–49.

SHERER, G. K. (1975). Tissue interaction in chick liver development: a reevaluation. I. Epithelial morphogenesis: the role of vascularity in mesenchymal specificity. *Devl Biol.* **46**, 281–295.

SLACK, J. M. W., DARLINGTON, B. G., HEATH, J. K. AND GODSAVE, S. F. (1987). Mesoderm induction in early *Xenopus* embryos by heparin-binding growth factors. *Nature* **326**, 197–200.

SMITH, S. M., PANG, K., SUNDIN, O., WEDDEN, S. E., THALLER, C. AND EICHELE, G. (1989). Molecular approaches to vertebrate limb morphogenesis. *Development* **107 Supplement**, 121–131.

SNOW, M. H. L. (1977). Gastrulation in the mouse: growth and regionalization of the epiblast. *J. Embryol. exp. Morph.* **42**, 293–303.

THEILER, K. (1989). *The House Mouse: Atlas of Embryonic Development*. Springer-Verlag, New York.

THOMAS, P. (1980). Hybridization of denatured RNA and small DNA fragments transferred to nitrocellulose. *Proc. natn. Acad. Sci. U.S.A.* **77**, 5201–5205.

THOMPSON, J. A., HAUDENSCHILD, C., ANDERSON, K. D., DIPIETRO, J. M., ANDERSON, W. F. AND MACIAG, T. (1989). Heparin-binding growth factor 1 induces the formation of organoid neovascular structures *in vivo*. *Proc. natn. Acad. Sci. U.S.A.* **86**, 7928–7932.

UNSICKER, K., REICHERT-PREIBSCH, H., SCHMIDT, R., PETTMANN, B., LABOURDETTE, G. AND SENSENBRENNER, M. (1987). Astroglial and fibroblast growth factors have neurotrophic functions for

cultured peripheral and central nervous system neurons. *Proc. natn. Acad. Sci. U.S.A.* **84**, 5459–5463.

VALLES, A. M., BOYER, B., BADET, J., TUCKER, G. C., BARRITAULT, D. AND THIERY, J. P. (1990). Acidic fibroblast growth factor is a modulator of epithelial plasticity in a rat bladder carcinoma cell line. *Proc. natn. Acad. Sci. U.S.A.* **87**, 1124–1128.

WALICKE, P., COWAN, W. M., UENO, N., BAIRD, A. AND GUILLEMIN, R. (1986). Fibroblast growth factor promotes survival of dissociated hippocampal neurons and enhances neurite extension. *Proc. natn. Acad. Sci. U.S.A.* **83**, 3012–3016.

WALICKE, P. A. AND BAIRD, A. (1988). Neurotrophic effects of basic and acidic fibroblast growth factors are not mediated through glial cells. *Devl Brain Res.* **40**, 71–79.

WILKINSON, D. G., BAILES, J. A., CHAMPION, J. E. AND MCMAHON, A. P. (1987). A molecular analysis of mouse development from 8 to 10 days post coitum detects changes only in embryonic globin expression. *Development* **99**, 493–500.

WILKINSON, D. G., BHATT, S. AND MCMAHON, A. P. (1989). Expression pattern of the FGF-related proto-oncogene *int*-2 suggests multiple roles in fetal development. *Development* **105**, 131–136.

WILKINSON, D. G., PETERS, G., DICKSON, C. AND MCMAHON, A. P. (1988). Expression of the FGF-related proto-oncogene *int*-2 during gastrulation and neurulation in the mouse. *EMBO J.* **7**, 691–695.

ZHAN, X., BATES, B., HU, X. AND GOLDFARB, M. (1988). The human FGF-5 gene encodes a novel protein related to fibroblast growth factors. *Molec. cell. Biol* **8**, 3487–3495.

*(Accepted 14 March 1991)*